



Published in final edited form as:

ACS Nano. 2013 November 26; 7(11): . doi:10.1021/nn4047925.

## Layer-by-Layer Nanoparticles for Systemic Codelivery of an Anticancer Drug and siRNA for Potential Triple-Negative Breast Cancer Treatment

Zhou J. Deng<sup>a,b</sup>, Stephen W. Morton<sup>a,b</sup>, Elana Ben-Akiva<sup>a,b</sup>, Erik C. Dreaden<sup>a,b</sup>, Kevin E. Shopsowitz<sup>a,b</sup>, and Paula T. Hammond<sup>a,b,\*</sup>

<sup>a</sup>Koch Institute for Integrative Cancer Research, Massachusetts Institute of Technology, Rm 76-553, Cambridge, MA 02139, USA

<sup>b</sup>Department of Chemical Engineering, Massachusetts Institute of Technology, Rm 76-553, Cambridge, MA 02139, USA

### Abstract

A single nanoparticle platform has been developed through the modular and controlled layer-by-layer process to co-deliver siRNA that knocks down a drug-resistance pathway in tumor cells and a chemotherapy drug to challenge a highly aggressive form of triple-negative breast cancer. Layer-by-layer films were formed on nanoparticles by alternately depositing siRNA and poly-L-arginine; a single bilayer on the nanoparticle surface could effectively load up to 3,500 siRNA molecules, and the resulting LbL nanoparticles exhibit an extended serum half-life of 28 hours. In animal models, one dose *via* intravenous administration significantly reduced the target gene expression in the tumors by almost 80%. By generating the siRNA-loaded film atop a doxorubicin-loaded liposome, we identified an effective combination therapy with siRNA targeting multidrug resistance protein 1, which significantly enhanced doxorubicin efficacy by 4 fold *in vitro* and led to up to an 8-fold decrease in tumor volume compared to the control treatments with no observed toxicity. The results indicate that the use of layer-by-layer films to modify a simple liposomal doxorubicin delivery construct with a synergistic siRNA can lead to significant tumor reduction in the cancers that are otherwise nonresponsive to treatment with Doxil or other common chemotherapy drugs. This approach provides a potential strategy to treat aggressive and resistant cancers, and a modular platform for a broad range of controlled multidrug therapies customizable to the cancer type in a singular nanoparticle delivery system.

### Keywords

Layer-by-layer nanoparticles; siRNA delivery; doxorubicin; triple-negative breast cancer; combination therapy

---

Triple-negative breast cancer (TNBC) is a subtype of breast cancer associated with very poor prognosis, but it currently has no standard-of-care therapy.<sup>1</sup> TNBC patients with residual disease after neoadjuvant chemotherapy experience significantly worse survival rates,<sup>2</sup> due to the ineffectiveness of chemotherapy to recurrent disease. This phenomenon is due to the high genetic diversity of tumor cells in this aggressive form of cancer, which are

---

\*Corresponding Author Department of Chemical Engineering, Massachusetts Institute of Technology, Rm 76-553, Cambridge, MA 02139, USA. Tel.: +1 617 258 7577; fax: +1 617 253 8557; Hammond@mit.edu.

Supporting Information. Additional figures, tables, results, and method description as described in the text. This material is available free of charge *via* the Internet at <http://pubs.acs.org>.

capable of evading treatment by overexpression of certain genes that involve anti-apoptotic or drug desensitizing pathways.<sup>3, 4</sup> siRNA holds great promise as a potential new class of targeted therapeutics with the ability of treating specific tumor types that have thus far been resistant to available therapies.<sup>5</sup> Combining genetic targeting of specific resistance pathways of tumor cells with the co-release of chemotherapy drugs can provide the ability to “turn off” or “switch” the tumor cell’s ability to fight, recover from, or avoid a given therapy, and thus greatly increase the treatment efficacy.

However, to create clinically relevant siRNA therapeutics for systemic treatment of advanced diseases, some key issues must be addressed: 1) prolonged nanoparticle persistence in circulation to allow sufficient access to the tumor for sustained therapy;<sup>5</sup> 2) high loading of siRNA per nanoparticle to overcome losses from the generally low uptake and endosomal escape rates in tumor cells;<sup>6, 7</sup> and, 3) the use of materials that can mediate endosomal escape of siRNA while minimizing potential toxicity.<sup>8</sup> Recent advances use materials such as block copolymers,<sup>9</sup> cyclodextrins,<sup>10</sup> copolypeptides, and charged lipids that are solid at body temperature.<sup>11</sup> Unfortunately, in many such polyplex or lipid formulations, it is difficult to control or alter key parameters for siRNA delivery, such as total number of siRNA molecules per particle and the relative ratio of siRNA to cationic polymer or lipid, which affects the therapeutic window. In fact, many polyplex and lipoplex systems are composed primarily of the lipid or cationic polymer used to package the siRNA, with polycation to siRNA molar ratios as high as 10 to 20:1, thus increasing the potential for toxic side effects and lowering the overall amount of siRNA that can be safely delivered systemically.<sup>10, 12–15</sup> Finally, most such complexes do not provide a means of combining chemotherapy drugs and inhibitors in a manner that may be synergistic, and controlling the relative siRNA:chemotherapy loading in a modular fashion.

Layer-by-layer (LbL) nanoparticles that utilize the process of sequentially depositing oppositely charged polymers to build a highly stable film with high siRNA content atop a nano-sized core provide an exciting new class of drug delivery platforms with promising clinical translational potential.<sup>16–18</sup> This approach allows precise control at nanometer-scale level to adapt a range of polycationic materials with siRNA loading and releasing, film stability, N-to-P ratio, transfection efficiency and cytotoxicity. The use of LbL nanoparticles for nanomedicine applications is a new and highly promising approach enabling the generation of modular nanoparticle systems;<sup>19</sup> however, only in the past 3–4 years have these systems been designed to exhibit desirable release properties *in vitro*, and fewer have been demonstrated *in vivo*, with the stability in plasma needed for efficient systemic delivery. A few researchers have shown that siRNA molecules can be incorporated into the outer coating of LbL nanoparticles,<sup>20–23</sup> although the current work has been heavily focused on inert gold nanoparticles, and this approach has not been adapted to the coating of active drug-loaded nanocarriers to achieve combination therapy. To achieve the clinical translational promise of this nanoscale technology, it is critical to adapt LbL nanoparticle methods to a broad range of materials, including biodegradable, low toxic biopolymers, and the most common and currently the most translational of nanocarriers—liposomes, which are already FDA approved for several forms of cancer and can be readily adapted to a number of chemotherapy approaches.

In order to further develop the LbL nanoparticles for systemic delivery to tumors in advanced diseases, we have recently demonstrated that the surface modification with LbL films can significantly improve the *in vivo* stability and pharmacokinetics of the nanoparticles for systemic drug delivery.<sup>17</sup> The LbL film can be further engineered to achieve active tumor targeting<sup>16</sup> and to modulate release rates of drugs from the nanoparticle cores,<sup>18</sup> which can increase the nanoparticle and drug bioavailability while mitigating any potential toxicity. Most attractive is the modular design of the LbL

nanoparticle platform, which provides the ability to introduce therapeutics in the core and in the surrounding layers of the film, thus creating an independently tunable multi-drug delivery device.

In this study, we sought to develop a combination therapeutic approach using LbL nanoparticles to treat an aggressive, chemo-resistant cancer cell type. By taking advantage of the modular design of the LbL nanoparticles, we have developed a novel codelivery system by building siRNA LbL films atop chemotherapy drug-loaded nanoparticles, as illustrated in Figure 1, followed by further functionalization of an exterior coat for “stealth” and tumor-targeting properties. We first screened a library of both synthetic and natural polycations to find the desired LbL film architecture on nanoparticles with high siRNA loading, stability and gene silencing efficiency, and low cytotoxicity. Upon a single-dose intravenous administration, the selected siRNA LbL nanoparticles achieved extended serum half-lives of up to 28 hours, much higher than typically reported half-lives of siRNA delivery nanoparticles.<sup>5, 24</sup> In a xenograft animal model of TNBC using MDA-MB-468 cells, a single dose injection of the siRNA LbL nanoparticles at 1 mg/kg was able to achieve a significant target gene silencing. Further, incorporation of a siRNA targeting a drug resistance pathway and a chemotherapy drug, doxorubicin, into a single LbL liposomal nanoparticle is demonstrated as a potent combination therapy in a TNBC xenograft model using MDA-MB-468 cells. This work highlights the potential of LbL nanoparticles as combination multi-therapeutic platforms for enhanced efficacy against aggressive cancer cell types.

## Results

### LbL nanoparticles as a modular and tunable platform for siRNA delivery

Initial work focused on developing multi-component delivery from LbL nanoparticle systems focused on the ability of the film to load and release therapeutics in an efficacious manner. To examine the ability to construct siRNA films on a nanoparticle template with high loading and low toxicity, we employed uniformly-sized, negatively charged carboxyl-modified polystyrene latex nanoparticles (CML) as a model nanoparticle core (120 nm in hydrodynamic size and  $-56$  mV in zeta potential) due to its similarity in size to many drug-loaded nanocarriers, such as liposomes.<sup>25, 26</sup> Several polycations were screened for the construction of siRNA LbL thin films, in alternation with the negatively charged siRNA; many of the materials considered in this study included native and synthetic polyamines, such as polypeptides, polyethyleneimine (PEI), chitosan and poly( $\beta$ -amino ester). Here, we identified poly-L-arginine (PLA) as a promising candidate for *in vivo* applications due to its high siRNA loading, film stability and silencing efficiency, and low cytotoxicity.

Deposition of PLA and siRNA on the nanoparticles was evidenced by the controlled increase of the nanoparticle hydrodynamic size of approximately 5 nm per layer (Figure 2A) and reversal of surface charge, as indicated by zeta potential characterization following deposition of each layer (Figure 2B). The uniformity of LbL deposition is evidenced by the maintenance of a low nanoparticle polydispersity following each layer (Figure 2C). The electron microscopic images revealed a core-shell structure of the siRNA LbL nanoparticles, confirming the uniform polymeric film coating the nanostructure (Figure 2D).

The loading of siRNA in the film was measured by subtracting the quantity of siRNA remaining free in solution after LbL deposition using picogreen® assays against a standard curve (Supporting Information Figure S1A, B). The PLA LbL film was able to load approximately 3,500 siRNA molecules per nanoparticle per layer, implying a conformal coating of siRNA on the nanoparticle with greater than 95% surface coverage (assuming  $6\text{nm} \times 2\text{nm}$  cross-sectional surface area per siRNA molecule).<sup>5</sup> The loading quantity was

further confirmed by using fluorescently-labelled siRNA and measuring the fluorescence intensity associated with the nanoparticles, and also by measuring the absorbance of siRNA at 260 nm (Supporting Information Figure S1C, D). In comparison, this loading was substantially greater than the PEI/siRNA LbL nanoparticles, which led to approximately 500 siRNA molecules per layer, and also greater than other reported polyplex systems.<sup>20, 27</sup> Further, we identified that there were approximately 2,300 molecules of PLA per layer on the nanoparticles. This number was estimated by the saturating stoichiometry of the surface charge (Supporting Information Figure S2). Based on this calculation, the N:P ratio in the PLA/siRNA LbL nanoparticles was found to be 1.7 (Supporting Information Table S1), which is much lower than other reported typical polyplex systems, which are typically from 8 to 30.<sup>20–23</sup> Importantly, a low N:P ratio will potentially allow higher amounts of the therapeutics to be delivered with less toxic effects.

Furthermore, it was found that the PLA/siRNA film was found to be stable at pH 7.4 in a physiologically relevant buffer (*i.e.* PBS) over an extended period of time, with less than 30% siRNA release over the first 24 hours (Figure 2E); this stability over the given timeframe is important, as it is undesirable to lose large amounts of the loaded siRNA during circulation prior to tumor access. As a modular system, increased siRNA loading can be easily achieved through the incorporation of additional bilayers of siRNA and polycation; in fact, we observed a linear increase in siRNA loading with numbers of layers (Figure 2F).

We next assessed the gene silencing efficiency and cytotoxicity of the siRNA LbL nanoparticles in green fluorescent protein (GFP)-expressing MDA-MB-468 cells. The surface of the nanoparticles was further coated by a layer of hyaluronic acid (HA), which has been previously reported for enhanced *in vivo* stability.<sup>17</sup> GFP-targeting siRNA were incorporated into the PLA/siRNA LbL nanoparticles, and a concentration-response study was carried out in comparison with PEI/siRNA LbL nanoparticles. PEI has been widely used for gene transfection *in vitro* due to its high transfection efficiency.<sup>14</sup> However, PEI is non-biodegradable and often exhibits unacceptable levels of cytotoxicity, making it difficult for *in vivo* use. Lower molecular weight PEI was reported to exhibit less cytotoxicity, however losing its capacity to complex siRNA.<sup>28</sup> Here, it was found that the PLA/siRNA LbL nanoparticles were able to achieve comparable levels of gene silencing compared to the PEI/siRNA (Figure 3A), while exhibiting no cytotoxicity at a concentration that was 20-fold higher (Figure 3B). Confocal microscopy images of dually-labelled siRNA and the CML core showed binding of the siRNA LbL nanoparticles to the cell membrane within 30 minutes of incubation. The co-localization of fluorescence suggested the integrity of the LbL nanoparticles in the extracellular environment. Over four hours of incubation, most of the nanoparticles were internalized into the cells, where siRNA dissociated from the CML cores and appeared diffuse throughout the cytoplasm, implying release of siRNA from the LbL film and endosomal escape (Figure 3C). To further test whether the gene silencing was recapitulated *in vivo*, a single dose of 1 mg/kg of the luciferase-targeting siRNA loaded in PLA/siRNA LbL nanoparticles were intratumorally injected into the luciferase-expressing MDA-MB-468 subcutaneous xenografts in NCR nude mice. Two days post-injection, using live animal bioluminescence imaging, a 2-fold decrease in luciferase activity was observed in the treated tumors compared to those injected with scrambled-siRNA LbL nanoparticles ( $n = 4$ ,  $P < 0.05$ ) (Figure 3D, E).

### Long-circulating LbL nanoparticles for systemic siRNA delivery to TNBC tumors in a xenograft model

To evaluate the pharmacokinetics of the PLA/siRNA LbL nanoparticles following systemic administration, AlexaFluor677 dye-labelled CML nanoparticles with the PLA/siRNA single bilayer LbL film architecture, terminated with HA (*i.e.* CML/PLA/siRNA/PLA/HA), were

administered into BALB/c mice *via* the tail vein. Quantification of recovered fluorescence at serial time points from blood isolated retro-orbitally generated the data shown in Figure 4A, which when fit to a two-compartment model is characterized by 0.06h (fast) and 27.8h (slow) half-lives. Live animal whole body fluorescence imaging further confirmed the stability of this nanoparticle system, as it was observed to persist in the animal for a prolonged period of time (12d) and was characterized in real-time by low levels of liver clearance (Figure 4B). Retention of the nanoparticles in the liver suggested the non-biodegradable nature of the polystyrene cores used in this particular model system, and would not be an issue for the drug-loaded biodegradable delivery systems investigated subsequently. There were no escalated levels of inflammatory cytokines, including IL-6, TNF, INF- $\gamma$ , IL-1 $\beta$  and IL-2, in the serum samples of the treated healthy BALB/c mice, suggesting these nanoparticles were not acutely immunogenic (Figure 4C, D). The notably long blood half-life of these systems was most likely attributed to the integrity of the LbL film *in vivo* and the “stealth” HA coat.<sup>17</sup> The biological performance of these systems is consistent with previous reports<sup>17, 18</sup> of LbL nanoparticles and provides an exciting platform for sustained systemic delivery of therapeutics. The siRNA molecules were stable in the nanoparticle coating with slow, sustained release over 72 hours in a physiologically relevant environment, suggesting stable incorporation of siRNA in the LbL film. As such, it was expected that the siRNA loaded largely co-localized with the nanoparticle substrate, validating the approach of fluorescently tracking the nanoparticle as a means of probing the pharmacokinetics of the therapeutic-containing system. Use of the model CML system thus informed the optimized LbL formulation for combination therapy with a drug-loaded liposomal core for TNBC targeting and treatment.

After observing the improved biological performance of these systems, we next sought to demonstrate the potential for these systems to traffic to solid tumors and induce knockdown following systemic administration. In NCR nude mice bearing luciferase-expressing MDA-MB-468 subcutaneous xenografts, luciferase-targeting siRNA LbL nanoparticles were intravenously administered at a single dose of 1.4 mg/kg. Quantitative RT-PCR analysis of the isolated tumor tissues 5 days post-injection revealed a 4-fold reduction in luciferase mRNA levels following luciferase siRNA treatment ( $n = 7$ ,  $P < 0.05$ ) (Figure 5A). Additionally, the knockdown of luciferase activity was found to be more profound at day 5 post-injection compared to day 3, implying a sustained rate of delivery and a cumulative effect of the siRNA in the tumors (Figure 5B). The significant target gene silencing can be attributed to the enhanced persistence of the LbL nanoparticles in blood, promoting increased access to the tumor and subsequent passive tumor localization through the enhanced permeation and retention effect as previously reported.<sup>29</sup> Moreover, HA is a well-known native ligand to CD44,<sup>30</sup> a surface marker of TNBC,<sup>31</sup> which could significantly promote the cellular uptake of the HA-coated LbL nanoparticles by the CD44 +ve MDA-MB-468 cells<sup>32</sup> (Supporting Information Figure S3). This was verified *in vitro* with the addition of free excess HA, where the uptake was largely attenuated, implicating HA-CD44 interactions as a means of cellular entry (Figure 5C, D). In addition, a fluorescently-labeled CML was deployed to track the tumor accumulation post *i.v.* injection, and the HA-coated LbL nanoparticles were found highly co-localized with the CD44 expression in the tumor tissue (Figure 5E). Together, the data suggests active targeting on the basis of CD44-mediated interactions with the HA-terminal layer. The result here demonstrates that a target gene within the tumor can be effectively silenced following a single, systemic administration of siRNA LbL nanoparticles.

### Codelivery of siRNA and doxorubicin using LbL liposomes as potential TNBC therapeutics

By combining siRNA that targets a drug resistance pathway and a chemotherapy drug into a single nanoparticle platform, we hypothesized that the efficacy of the chemotherapy drug

will be significantly enhanced.<sup>3</sup> Thus, we developed a combination chemotherapy drug-siRNA delivery platform using LbL nanoparticles, in which we built siRNA-loaded LbL films onto doxorubicin-loaded negatively-charged phospholipid liposomes (Figure 6A). We carefully characterized the physicochemical properties of the LbL-coated liposomes, and have found that the change in size, surface charge, film thickness and polydispersity during the LbL coating process was similar to that of LbL-coated CML nanoparticles (Supporting Information Figure S4). Our data here suggested that we successfully adapted the CML nanoparticles as a model and were able to translate the LbL process to the liposome system. This success was likely due to the similarity in size, surface charge and shape between the CML nanoparticles and the liposomes (*i.e.* averagely 120 nm in diameter with zeta potential of -55 mV). These properties dictate the surface interactions of the nanoparticles with polymeric materials and the formation of the LbL film on the surface, and eventually, the biological outcomes of the nanoparticles. Evidently, we found that LbL liposomes exhibited long circulation time, similar to that of the LbL CML nanoparticles (Supporting Information Figure S4). We sought to use liposomes as the core for the LbL nanoparticles, due to their wide use as approved drug carriers and success in Doxil™ for breast cancer treatment.<sup>33-35</sup> The liposomes exhibit high *in vivo* stability with controlled drug release,<sup>33-35</sup> providing a stable nano-sized core for building the long-circulating LbL film. The loading efficiency and the loading percentage of doxorubicin in the liposomes were 97 % and 5.5 % w/w, while each PLA/siRNA bilayer provided 3,500 siRNA molecules per liposome. We generated core-shell siRNA LbL liposomes with a siRNA-to-doxorubicin molar ratio of 1:25, or mass ratio of 1:1. The LbL liposomal formulation exhibited extended stability in tissue culture medium with less than 20% release of each therapeutic component over a period of 24 hours, while the two components showed staggered release over 72 hours with a faster release rate of siRNA from the film, comparing to the drug from the liposome core.(Figure 6B).

To identify a combination gene target to doxorubicin, we first screened a small library of siRNA targets for doxorubicin codelivery by preparing siRNA/doxorubicin LbL liposomes and examining the efficacy of the nanoparticle treatments in MDA-MB-468 cells *in vitro*. The siRNAs were selected to target drug efflux (multidrug resistance protein 1 (MRP1)), antiapoptotic (Bcl2, EGFR) and oncogenic (c-myc) pathways (Supporting Information Figure S5). From this data, it was found that the MRP1 was most efficacious in combination with doxorubicin. MRP1 siRNA was found to significantly enhance the efficacy of liposomal doxorubicin *in vitro*, as shown by a 4.5-fold decrease in IC<sub>50</sub> values from the scrambled siRNA control (IC<sub>50</sub> = 9 μm) to the combination siRNA/doxorubicin liposome treatment (IC<sub>50</sub> = 2 μM) (Figure 6C). MRP1 is a cell-surface efflux pump involved in redox regulation of multidrug resistance by reducing the intracellular concentration of xenobiotics or drugs, and is a clinically relevant biomarker associated with the poor prognosis of TNBC.<sup>36</sup> Combination therapy of MRP1 siRNA and doxorubicin has been reported to increase the doxorubicin accumulation in tumor cells and therefore to enhance efficacy.<sup>13</sup>

In a proof-of-concept study, we treated NCR nude mice bearing subcutaneous xenograft tumors of luciferase-expressing MDA-MB-468 cells with intravenous administration of MRP1 siRNA/doxorubicin liposomes. The controls included the LbL doxorubicin liposomes that were loaded with scramble-sequenced siRNA, the empty LbL liposomes loaded with MRP1 siRNA and a saline-treated group. The mice were treated every 5 days for 15 days, for a total of 3 tail vein injections at 1 mg/kg of doxorubicin and 1 mg/kg siRNA, and the tumor volumes were monitored through bioluminescence of the luciferase activities of the tumors over the course of the treatment (Figure 7A, Supporting Information Figure S6); thus the measured bioluminescence represents a quantitative measure of the size of the tumor. Compared to caliper measurements that can be sensitive to experimental technique, bioluminescence provides a measure of the tumor size with reduced experimental bias and

errors.<sup>37</sup> Significant tumor regression was seen in the combination treatment group, which decreased the average tumor volume by 4- and 8-fold compared to the scramble control and the saline control, respectively ( $n = 6-8$ ,  $p < 0.05$ ) (Figure 7B). In some of the animals treated with combo therapy, complete tumor regression was observed. MRP1 siRNA-only treatment did not show any tumor inhibitory effects. Quantitative RT-PCR analysis of mRNA isolated from tumor tissues revealed the MRP1 LbL liposomes significantly decreased the MRP1 mRNA level in the tumor tissues compared to the scramble control ( $n = 8$ ,  $p < 0.05$ ) (Figure 7C). The knockdown was confirmed by immunohistochemical staining of MRP1 protein in the tumor tissue, where treated tumor tissue showed marked decreases in protein expression across the tissue section, compared to the samples from the saline-treated control groups (Figure 7D, E). In addition, histology (Figure 7F, G) and serum biochemistry (Table 1) analyses of mouse tissues collected at the end of the experiment showed no sign of liver or kidney damage, suggesting the LbL nanoparticle treatments were apparently not toxic at the administered dose.

## Discussion

Patients with recurrent forms of TNBC are typically not responsive to doxorubicin therapy alone; however, reversing or lowering the resistance of the cancer to the doxorubicin treatment provides a powerful platform for improved therapeutic outcomes.<sup>38, 39</sup> The concept of combination delivery of siRNA and an anticancer drug in a single delivery platform, such as in a nanoparticle, has recently shown promising preliminary results to restore or enhance drug efficacy in a number of animal studies of lung and breast cancers.<sup>12, 13, 28</sup> In this study, we developed a novel LbL nanoparticle-based platform for systemic codelivery of siRNA and an anticancer drug, specifically to lower the drug resistance with MRP1-targeting siRNA to increase the potency of the doxorubicin against MDA-MB-468 cells. In this paper, we establish that LbL nanoparticles can be used to combine siRNA and chemotherapy agents within a single delivery vehicle, and that such systems can be delivered systemically to target tumors, enabling time-dependent knock-down of a drug resistant gene, followed by tumor treatment. Through modular design, we developed a codelivery platform by generating siRNA-loaded LbL films atop a doxorubicin-loaded liposome with an exterior negatively-charged phospholipid membrane amenable to LbL deposition. By combining different therapeutics into a single delivery vehicle with a controlled, staggered release profile, the LbL nanoparticle therapeutics were able to achieve synergistic targeting to tumors, while minimizing toxicity. The combination system demonstrates the potency of delivery of siRNA using this method, as indicated by a significant degree of knockdown achieved *in vivo*, and the efficacy of dual delivery, which promoted tumor regression, and in some cases led to complete tumor shrinkage, in sharp contrast to results observed with doxorubicin alone, which exhibited much lower efficacy.

In this study, we have demonstrated the capability of LbL nanoparticles as a modular platform for effective delivery of diverse classes of therapeutics, including chemotherapy drugs and siRNA. Key to achieving a modular system is use of clinically relevant materials. Thus, we carefully selected polymeric materials, such as PLA and HA for high loading, high transfection efficiency and biostability, and low cytotoxicity, while deploying liposomes, a well established class of drug carriers. In this proof-of-principle study, we demonstrated that we could assemble these different components through a highly controlled LbL engineering approach. By incorporating siRNA into the nano-scale thin films on top of a nanoparticle, we are able to achieve significant target gene silencing in tumor tissues upon a single-dose intravenous administration. This is attributed to a delivery vehicle that enables a) high siRNA loading, b) extended serum half life that allows for prolonged exposure of the tumor to the treatment, c) active targeting and tumor cell uptake *via* HA-CD44 mediated

interactions, d) effective endosomal escape, and e) minimum toxicity by biodegradable materials.

First, the loading of the siRNA in the LbL film is tunable with up to 3,500 siRNA molecules per layer, which suggests an almost conformal coat of siRNA molecules. In some of the most recent efforts to better understand the intracellular trafficking for siRNA delivery, microscopy-based imaging studies were conducted to track the siRNA and its carriers inside the cells. These experiments revealed that endosomal escape is an extremely rare event with only 1–2% of nanoparticles<sup>6, 7</sup> accessing the cytoplasmic compartment, where the therapeutically relevant concentrations of siRNA could be as low as between 2,000–4,000 copies.<sup>6</sup> These studies implied that the loading of 3,500 siRNA molecules per PLA/siRNA LbL nanoparticle could achieve desired levels of gene silencing with potentially a single event of successful intracellular delivery. Besides the high loading, the siRNA LbL nanoparticles consist of much lower amounts of polycationic materials in relation to the loaded siRNA. In a brief summary (Supporting Information Table S2), we compared the N:P ratio and siRNA loading of the LbL nanoparticle system with other recently reported polyplex systems. It was found that the polyplex systems consist predominately of the cationic polymer used as a carrier, with an average N:P ratio greater than 10, and as high as 30. In comparison, the amount of the polycationic materials in the LbL nanoparticle system is greatly minimized, with an almost stoichiometric ratio of polycation to the loaded siRNA; our PLA/siRNA LbL nanoparticles achieved an N:P ratio of 1.7. This low N:P ratio is believed to be important for reducing the level of potential toxic effects and thus maximizing the therapeutics to be delivered.

Second, the HA outer shell is able to provide a “stealth” surface<sup>17, 40</sup> for prolonged circulation with serum half-life of the nanoparticles up to 28 hours on the LbL CML nanoparticles. We have also previously reported that HA coat promotes passive tumor targeting through the EPR effect on the LbL gold nanoparticles and quantum dots.<sup>29</sup> Furthermore, as a native ligand to CD44, a marker overexpressed in TNBC tumors,<sup>31</sup> HA is able to further mediate the cellular uptake of the nanoparticles through receptor-mediated interactions. Together, HA provides a promising surface layer for systemic delivery to CD44 +ve tumors, informing its incorporation as the terminal layer on the LbL liposomal system. Although there are certain differences in physicochemical properties between the latex nanoparticles and liposomes, it was expected that the hyaluronic acid coated liposomes would possess the same desired long-circulating characteristics, given that liposomes are stable, first-in-clinic delivery vectors with controlled drug release profiles, as well as the understanding that surface properties largely dictate the biological interactions and *in vivo* stability of nanoparticles.<sup>41–44</sup> Most importantly, significant tumor targeting and target gene silencing was observed for both siRNA-loaded latex nanoparticles and liposomes, suggesting that we were successful in translating the design from the model system to a drug-loaded system.

Third, the modular design of the LbL film architecture allows us to select desired materials with biodegradability and low toxicity to facilitate the clinical translation. In a preliminary investigation, we have screened a library of polycations for constructing a desired siRNA LbL film on nanoparticles, and have found that the chemistry,  $pK_a$  values, charge density, and structure of the polycations play major roles in determining the siRNA loading capacity, film stability, release profiles and film thickness of the LbL nanoparticles. Here, we have selected the biodegradable polypeptide PLA due to its ability to load a large number of siRNA molecules in the LbL films with high stability, high silencing efficiency, and little cytotoxicity. PLA- or arginine-rich polypeptide/polymer-based siRNA delivery vehicles have been previously reported to provide promising endosomal escape capacity,<sup>15, 45, 46</sup> as arginine contains a permanently positively charged guanidinium group that facilitates the



intracellular delivery through a potential membrane disruptive mechanism.<sup>47, 48</sup> By using biodegradable materials, the delivery system was able to bypass the challenge of freeing siRNA from the polyplex after endosomal escape, which is often observed in the PEI-based delivery systems.<sup>8</sup> In the meantime, by using biodegradable polypeptide-based nanoparticles, such as PLL, Koo *et al.* reported a controlled release rate of the siRNA with prolonged gene silencing for more than 3 weeks.<sup>21</sup>

Furthermore, recent investigations in our lab and others have described scalable approaches to the manufacture of LbL nanoparticles using spray layer-by-layer<sup>49</sup> or electrophoresis methods.<sup>50</sup> Together, these state-of-art manufacture methods allow the LbL nanoparticle technology to be adapted to large-scale markets, while maintaining modularity, ease of design, reproducibility and fabrication.

## Conclusion

By generating a nanolayered siRNA-loadable LbL film onto a drug-loadable nanoparticle, we have developed a novel drug delivery platform that is modular and can be tailored to achieve high loading of therapeutics, intracellular delivery, extended serum half-life and tumor targeting. We have demonstrated its capability for combination therapy by co-delivering siRNA that targets MRP1, a drug efflux pump and doxorubicin to treat TNBC in animal models, and seen significantly enhanced efficacy. Furthermore, we have generated a clinically translational system by deploying a combination of biodegradable biopolymers and FDA-approved liposomes. In summary, the results here provide a potential strategy to treat an aggressive and recurrent form of TNBC, as well as a means of adapting this platform to a broad range of controlled multi-drug therapies customizable to the cancer type in a singular nanoparticle delivery system.

## Methods

### Materials

Carboxylic modified latex (CML) polystyrene nanoparticles were purchased from Invitrogen. All lipid components were purchased from Avanti Polar Lipids, except for cholesterol from Sigma. Doxorubicin was purchased from LC laboratories. CCK-8 cell proliferation assay kit was purchased from Sigma-Aldrich. All siRNAs, including MRP1 5'-GGCUACAUCAGAUGACACdTdT-3', firefly luciferase 5'-CGUACGCGAAUACUUCGAdTdT-3', GFP 5'-GCAAGCUGACCCUGAAGUUCAUdTdT-3', and scrambled control 5'-UUCUCCGAACGUGUCACGUDdTdT-3' were custom-synthesized and purchased from Dharmacon. DNA primers, including MRP1 (forward 5'-ATGTCACGTGGAATACCAGC-3', reverse 5'-GAAGACTGAACTCCCTTCCT-3'), firefly luciferase (forward 5'-CAACTGCATAAGGCTATGAAGAGA-3', reverse 5'-ATTTGTATTACGCCATATCGTTT-3'),  $\beta$ -actin (forward 5'-TGAGCGGGCTACAGCTT-3', reverse 5'-TCCTTAATGTCACGCACGATTT-3') were purchased from Integrated DNA Technologies. Monoclonal antibodies, including anti-CD44 (IM7), anti-MRP1 (QCRL-1) and the IgG isotype control antibody were purchased from Santa Cruz Biotechnologies. Dulbecco's modified eagle's medium (DMEM), fetal bovine serum, penicillin/streptomycin, L-glutamine and RNase-free deionized water were purchased from Invitrogen. Hyaluronic acid 200 kDa was purchased from Lifecore Biomedical. All other materials, including polymers (poly-L-arginine, 10 kDa and 40 kDa; PEI 25 kDa), chemicals (dibasic sodium phosphate, citric acid, sodium citrate, sodium carbonate) and solvents (chloroform, methanol, phosphate buffered saline) were furnished by Sigma. All chemicals were reagent grade. All polymer and buffer solutions were filtered with a 0.2  $\mu$ m pore size polycarbonate syringe filter before use.

### Preparation of siRNA LbL nanoparticles

The protocol of siRNA LbL nanoparticle preparation was developed based on the previously established method.<sup>17</sup> Briefly, the negatively charged cores used were either carboxyl modified latex (CML) nanoparticles (120 nm in hydrodynamic size; -55 mV; with or without AlexaFluor677 dye; Invitrogen) or phospholipid functionalized liposomes (see section below for synthesis). For LbL assembly, nanoparticles at 1 mg/ml were first mixed with 50 µg/ml polycations (PLA, 10 kDa; or PEI, 25 kDa) in RNase-free deionized water. The mixing was facilitated by a brief period of bath sonication (3–5 seconds), followed by a washing step through centrifugation (30,000 g, 30 minutes for CML nanoparticles; 15,000 g, 15 minutes for liposomes). To incorporate siRNA, purified nanoparticles were mixed with a siRNA solution prepared at 4 µM in water, followed by further purification. This step could be repeated to achieve desired siRNA loading. Typically, the purified polycation/siRNA nanoparticles were further mixed with hyaluronic acid (200 kDa) at a concentration of 1 mg/ml in a pH 7.4 solution containing 100 nM dibasic sodium phosphate, followed by purification.

### Preparation of Liposomes

Liposomes were formulated at a mass ratio of 56:39:5 (DSPC:Cholesterol:POPG). These three components were dissolved in a 2:1 mixture of chloroform:methanol. A thin film of these materials was generated by rotary evaporation at 40°C, 150 mbar. This film was allowed to desiccate overnight for complete drying. Hydration of the lipid film was conducted at 65°C under sonication in 300 mM citric acid buffer (pH 4) for 1 hour, after which they were filtered through a 0.2 µm PES syringe filter and allowed to cool to room temperature. The pH of the liposomal suspension was then adjusted to 6.5 by addition of 300 mM sodium carbonate buffer to create a gradient between the exterior and interior compartments. Doxorubicin at a feed ratio of 3 mg drug:50 mg lipids was then added in a 0.9% sodium chloride solution to load *via* a pH gradient method. The final drug-loaded system was subsequently purified out of the high salt buffers and any excess, unloaded drug *via* centrifugal filtration (100 K MWCO Millipore) and transferred to phosphate buffered saline.

### Physicochemical characterization

All size, zeta potential and polydispersity index measurements were made using a Malvern ZS90 zeta-sizer. For TEM imaging, nanoparticle solutions were drop-cast onto carbon coated copper grids without any staining. The loading of siRNA on the LbL nanoparticles was examined by 1) measuring the free siRNA in the supernatant using Picogreen assay (Invitrogen) against a dsRNA standard curve; 2) by absorbance of the supernatant at 260 nm using NanoDrop (NanoDrop, Inc.); or 3) using a fluorescent dye labelled siRNA and measuring the nanoparticle-associated fluorescent against a fluorescent siRNA standard curve. The stability of the siRNA LbL films on nanoparticles were examined in PBS or in phenol-free DMEM at room temperature. The amount of siRNA released into the supernatant over different incubation time points was measured by picogreen assays. The release of doxorubicin from liposomes was examined by incubating nanoparticle under depletion conditions (1 L buffer for 1 mL NP suspension) in phosphate buffered saline (PBS) under agitation in 1 mL 3.5 K MWCO float-a-lyzers (Spectrum) at room temperature. PBS was replenished each day of the experiment. Samples were taken of the liposomes remaining to quantify remaining doxorubicin concentrations by absorbance at 480 nm.

### *in vitro* experimentation

MDA-MB-468 triple-negative breast adenocarcinoma cells (ATCC) were used in our experiments and grown in DMEM media supplemented with 10% fetal bovine serum, 50

units/mL penicillin and 50 units/mL streptomycin. Stable GFP- and firefly luciferase-over expressing MDA-MB-468 cells were established using lentivirus vectors (Cell Biolabs, Inc.) according to the manufacturer's protocols.

Gene silencing of siRNA LbL nanoparticles was assessed in GFP-overexpressing MDA-MB-468 cells. Briefly, the cells were seeded on a 96-well plate overnight at 30% confluence, and treated with increasing concentrations of LbL nanoparticles, of which the amounts were normalized to the siRNA loading. The cells were treated with GFP-targeting siRNA LbL nanoparticles, and compared with scrambled control siRNA nanoparticles. Three days after the treatments, the cells were trypsinized and the cell-associated GFP fluorescence (excitation 480 nm; emission 530 nm) was analyzed using a BD LSRFortessa flow cytometer coupled with a high-throughput system for the 96-well plate format (BD biosciences, San Jose, CA).

Cytotoxicity assays were performed using CCK-8 cytotoxicity assay (Sigma). Briefly, cells were firstly seeded in a 96-well plate at 30% confluence for 24 hours and treated with the nanoparticles at various concentrations. After 3 days of incubation, the cells were replaced in fresh serum-free OptiMEM media containing 10% v/v of the CCK-8 proliferation reagent. After 2 hour incubation at 37°C, the absorbance at 450 nm was measured by a plate reader. Cell viabilities were normalized to an untreated control and calculated using a standard curve. To study the efficacy of siRNA/doxorubicin LbL nanoparticles, the data were fit with a dosedependent inhibition curve using Prism 5 (GraphPad).

Cellular uptake of nanoparticles was assessed by confocal microscopy and flow cytometry. The confocal microscopic images were taken using a Nikon A1R Ultra-Fast Spectral Scanning Confocal Microscope (Nikon instruments Inc., Melville, NY). Briefly, cells were seeded in CELLview glass bottom dish (Greiner Bio-One GmbH, Germany) at  $1 \times 10^5$  cells per well and grown overnight. Cells were then incubated with nanoparticles at 37°C. At the end of this period, cells were washed followed by addition of DAPI for an additional 10 minutes, after which they were washed and imaged. The quantity of uptake was measured by flow cytometry. Briefly, the cells were seeded in a 96-well plate at 80% confluence overnight, and treated with fluorescently labelled nanoparticles at 100 µg/ml for various periods of time at 37°C, followed by washing and trypsinization. The cell-associated fluorescence was analyzed by a BD LSRFortessa flow cytometer coupled with a high-throughput system for the 96-well plate format (BD Biosciences).

### ***in vivo* experimentation**

Female BALB/c and NCR nude mice (4–6 weeks old) were purchased from Taconic and the AIN-93 purified diet was from PharmaServ/Testdiets. Mice were kept on the AIN-93 diet for at least a week before experimentation to reduce levels of body auto-fluorescence. All *in vivo* experimentation was carried out under the supervision of the Division of Comparative Medicine (DCM), Massachusetts Institute of Technology, and in compliance with the Principles of Laboratory Animal Care of the National Institutes of Health. Cell lines were purchased from ATCC and were tested routinely for pathogens before use in animals *via* DCM.

Pharmacokinetics of LbL nanoparticles were investigated in BALB/c female mice (Taconic) through intravenous administration (*i.e.* tail vein injection) of scrambled siRNA LbL nanoparticles with AlexaFluor677 labelled cores at a siRNA concentration of 1 mg/ml in 0.1 ml. The corresponding radiant efficiency was adjusted to  $1 \times 10^{10}$  by the IVIS whole-animal imaging system (Xenogen, Caliper Instruments). Whole-animal fluorescence imaging was performed at the indicated time points for one cohort of mice ( $n = 3$ ), while a separate cohort was used for retro-orbital bleeds to determine the circulation serum half-life of the

nanoparticles. Imaging and circulation data presented is normalized to auto-fluorescence obtained prior to injection. Analysis of circulation data based on recovered fluorescence normalized to pre-injection blood auto-fluorescence is displayed with a two-compartment model fit with both slow and fast half-lives presented.

Immunogenicity of siRNA LbL nanoparticles in healthy BALB/c mice was examined using the blood samples collected during the pharmacokinetics studies mentioned above. Cytokines in serum, including IL-6, IL-2, IL-1 $\beta$ , TNF and IFN- $\gamma$  were determined using a cytometric bead array kit (BD Biosciences) according to the manufacturer's instruction.

Subcutaneous xenograft tumors of TNBC models were induced by seeding of firefly luciferase-overexpressing MDA-MB-468 in each rear hind flank of NCR nude mice. Briefly, cells were mixed in a 1:1 ratio with BD Matrigel™ Basement Membrane Matrix to a final density of  $5 \times 10^7$  cells/0.1 ml. The matrix-cell suspension of 0.1 ml was injected in each rear hind flank of NCR nude mice. Tumors were allowed to grow to 100 mm<sup>3</sup> before experimentation.

LbL nanoparticle treatments in the mouse models were performed by intratumorally or intravenously administering the LbL nanoparticles in 0.1 ml injections at selected concentrations. In the intratumoral treatment experiments, 4 tumor-bearing mice were treated with luciferase-targeting siRNA LbL nanoparticles or scrambled siRNA LbL nanoparticles at 1 mg/kg siRNA by intratumoral injection at either site of the flanks. The luciferase activities in the tumors were monitored by bioluminescence pre- and 2 days post-injection. The images were obtained by 0.1 ml intraperitoneal injections of 30 mg/kg D-luciferin (Caliper) and were recorded with an open luminescence filter 15 minutes post-injection. In the single-dose systemic delivery experiment, tumor-bearing mice were randomly divided into 2 groups, 7 animals per group, and were treated with luciferase-targeting siRNA LbL nanoparticles or scrambled siRNA LbL nanoparticles at 1.4 mg/kg siRNA. The luciferase activities in the tumors were monitored by bioluminescence pre-, 3 days and 5 days post-injection. In the tumor growth inhibition experiment, tumor-bearing mice were randomly divided into 4 groups, 8 animals per group. These groups were used for comparing the effects of saline, MRP1 siRNA LbL liposomes with no doxorubicin, scrambled siRNA LbL doxorubicin liposomes and MRP1 siRNA LbL doxorubicin liposomes, respectively. The nanoparticle treatment and control groups received intravenous administration of LbL nanoparticles at a dose equivalent to 1 mg/kg doxorubicin and/or 1 mg/kg siRNA, given the mass ratio of doxorubicin to siRNA was loaded at 1:1 in the LbL nanoparticles. The saline control group received intravenous administration of 0.1 ml PBS. The mice were dosed repeatedly over 10 days of treatment for a total of 3 doses. The tumor sizes were monitored through bioluminescence pre- and post-treatments every 5 days for up to 15 days. All the above data were presented, along with region of interest quantification of radiance corresponding to the xenograft-specific luminescence for each mouse treated. Data was normalized for each mouse against the tumor luminescence prior to injection and presented as fold luminescence above this measurement. At the end of the experiments, the tumor tissues were harvested and randomly spliced into a few sections for further analyses.

qPCR analyses of target gene silencing were performed by isolating total RNA from the sliced tissues using PARIS® kit (Invitrogen) according to the manufacturers' protocol. The cDNA was synthesized using iScript™ cDNA synthesis kit (Bio-Rad Laboratories). qPCR was performed using iQ SYBR Green Supermix (Bio-Rad Laboratories) along with selected DNA primer pairs. Experiments were performed in triplicates. PCR amplification was performed by incubation at 95°C for 10 minutes, followed by 40 cycles of 95°C for 15 seconds and 60°C for 1 minute (LightCycler® 480 system, Roche). The relative gene

expression was analyzed using the delta-delta Ct method and normalized using  $\beta$ -actin as a housekeeping gene.

Immunohistochemistry was performed using fixed, paraffin-embedded tumor sections of 5-micron thickness. The MRP1 (1:50 dilution) staining was performed by the histology facility at MIT. Immunostaining images were examined under a light microscope (Nikon). The CD44 was stained by a FITC-conjugated anti-CD44 antibody and the slides were examined using a confocal fluorescence microscope.

*in vivo* toxicity of the LbL nanoparticle treatments were assessed using serum and organ tissue samples isolated from both the treated and control mice at the end of the experiment. Blood biochemistry of liver and kidney panels was analysed by Charles River Laboratories. Liver and kidney tissues were fixed and sectioned for H&E staining. Images were collected using a Nikon light microscope.

### Statistical Analysis

Experiments were performed in triplicates, or otherwise indicated. Data were analyzed using descriptive statistics, single-factor analysis of variance (ANOVA), and presented as mean values  $\pm$  standard deviation (SD) from three to eight independent measurements. Statistical comparisons between different treatments were assessed by two-tailed t tests or one-way ANOVA assuming significance at  $P < 0.05$ .

### Supplementary Material

Refer to Web version on PubMed Central for supplementary material.

### Acknowledgments

We would like to thank funding from the Janssen Pharmaceuticals, Inc. TRANSCEND grant, as well as support, in part, by the Koch Institute Support (core) Grant P30-CA14051 from the National Cancer Institute. We would also like to thank the Koch Institute for Integrative Cancer Research at MIT for providing facilities to support this work, as well as DCM (Department of Comparative Medicine, MIT) and the Koch Institute Swanson Biotechnology Center for assistance with animal experiments and facilities, especially the microscopy, flow cytometry and histology cores. J.Z.D. would like to acknowledge a CJ Martin Fellowship supported by National Health and Medical Research Council, Australia. S.W.M. would like to acknowledge a National Science Foundation Graduate Research Fellowship (NSF GRF). K.E.S. would like to acknowledge a National Sciences and Engineering Research Council (NSERC) postdoctoral fellowship. The authors wish to dedicate this paper to the memory of Officer Sean Collier, for his caring service to the MIT community and for his sacrifice.

### REFERENCES

1. Kassam F, Enright K, Dent R, Dranitsaris G, Myers J, Flynn C, Fralick M, Kumar R, Clemons M. Survival Outcomes For Patients With Metastatic Triple-Negative Breast Cancer: Implications For Clinical Practice And Trial Design. *Clin. Breast Cancer*. 2009; 9:29–33. [PubMed: 19299237]
2. Liedtke C, Mazouni C, Hess K, André F, Tordai A, Mejia J, Symmans W, Gonzalez-Angulo A, Hennessy B, Green M, et al. Response To Neoadjuvant Therapy And Long-Term Survival In Patients With Triple-Negative Breast Cancer. *J. Clin. Onco*. 2008; 26:1275–1281.
3. Lee MJ, Ye AS, Gardino AK, Heijink AM, Sorger PK, MacBeath G, Yaffe MB. Sequential Application Of Anticancer Drugs Enhances Cell Death By Rewiring Apoptotic Signaling Networks. *Cell*. 2012; 149:780–794. [PubMed: 22579283]
4. Natarajan K, Xie Y, Baer MR, Ross DD. Role Of Breast Cancer Resistance Protein (Bcrp/abcg2) In Cancer Drug Resistance. *Biochem. Pharmacol.* 2012; 83:1084–1103.
5. Whitehead KA, Langer R, Anderson DG. Knocking Down Barriers: Advances In siRNA Delivery. *Nat. Rev. Drug Discov*. 2009; 8:129–138. [PubMed: 19180106]

6. Gilleron J, Querbes W, Zeigerer A, Borodovsky A, Marsico G, Schubert U, Manygoats K, Seifert S, Andree C, Stoter M, et al. Image-Based Analysis Of Lipid Nanoparticle-Mediated Sirna Delivery, Intracellular Trafficking And Endosomal Escape. *Nat. Biotechnol.* 2013; 31:638–646. [PubMed: 23792630]
7. Rehman Z, Hoekstra D, Zuhorn I. Mechanism of Polyplex- and Lipoplex-Mediated Delivery of Nucleic Acids: Real-Time Visualization of Transient Membrane Destabilization without Endosomal Lysis. *ACS Nano.* 2013; 7:3767–3777. [PubMed: 23597090]
8. Bonner D, Leung C, Chen-Liang J, Chingozha L, Langer R, Hammond P. Intracellular Trafficking Of Polyamidoamine-Poly(Ethylene Glycol) Block Copolymers In Dna Delivery. *Bioconjug. Chem.* 2011; 22:1519–1525. [PubMed: 21761838]
9. Sun TM, Du JZ, Yao YD, Mao CQ, Dou S, Huang SY, Zhang PZ, Leong KW, Song EW, Wang J. Simultaneous Delivery of siRNA and Paclitaxel *via* a “Two-in-One” Micelleplex Promotes Synergistic Tumor Suppression. *ACS Nano.* 2011; 5:1483–1494. [PubMed: 21204585]
10. Zuckerman JE, Choi CHJ, Han H, Davis ME. Polycation-Sirna Nanoparticles Can Disassemble At The Kidney Glomerular Basement Membrane. *Proc. Natl. Acad. Sci. U.S.A.* 2012; 109:3137–3142. [PubMed: 22315430]
11. Lobovkina T, Jacobson GB, Gonzalez-Gonzalez E, Hickerson RP, Leake D, Kaspar RL, Contag CH, Zare RN. In Vivo Sustained Release of siRNA from Solid Lipid Nanoparticles. *ACS Nano.* 2011; 5:9977–9983. [PubMed: 22077198]
12. Zhang Y, Schwerbrock N, Rogers A, Kim W, Huang L. Codelivery of VEGF siRNA and Gemcitabine Monophosphate in a Single Nanoparticle Formulation for Effective Treatment of NSCLC. *Mol. Ther.* 2013; 21:1559–1569. [PubMed: 23774791]
13. Taratula O, Kuzmov A, Shah M, Garbuzenko O, Minko T. Nanostructured Lipid Carriers As Multifunctional Nanomedicine Platform For Pulmonary Co-Delivery Of Anticancer Drugs And siRNA. *J. Controlled Release.* 2013
14. Nimesh S. Polyethylenimine As A Promising Vector For Targeted Sirna Delivery. *Curr. Clin. Pharmacol.* 2012; 7:121–130. [PubMed: 22432843]
15. Won YW, Yoon SM, Lee KM, Kim YH. Poly(oligo-D-arginine) With Internal Disulfide Linkages as a Cytoplasm-sensitive Carrier for siRNA Delivery. *Mol. Ther.* 2011; 19:372–380. [PubMed: 21081902]
16. Poon Z, Chang D, Zhao XY, Hammond PT. Layer-by-Layer Nanoparticles with a pH-Sheddable Layer for in Vivo Targeting of Tumor Hypoxia. *ACS Nano.* 2011; 5:4284–4292. [PubMed: 21513353]
17. Poon Z, Lee JB, Morton SW, Hammond PT. Controlling in Vivo Stability and Biodistribution in Electrostatically Assembled Nanoparticles for Systemic Delivery. *Nano Lett.* 2011; 11:2096–2103. [PubMed: 21524115]
18. Morton SW, Poon Z, Hammond PT. The Architecture And Biological Performance Of Drug-Loaded Lbl Nanoparticles. *Biomaterials.* 2013; 34:5328–5335. [PubMed: 23618629]
19. Hammond PT. Polyelectrolyte Multilayered Nanoparticles: Using Nanolayers For Controlled And Targeted Systemic Release. *Nanomedicine (Lond.).* 2012; 7:619–622. [PubMed: 22630144]
20. Elbakry A, Zaky A, Liebk R, Rachel R, Goepferich A, Breunig M. Layer-by-Layer Assembled Gold Nanoparticles for siRNA Delivery. *Nano Lett.* 2009; 9:2059–2064. [PubMed: 19331425]
21. Seung Koo L, Ching-Hsuan T. A Fabricated siRNA Nanoparticle for Ultralong Gene Silencing In Vivo. *Adv. Funct. Mater.* 2013; 23:3488–3493.
22. Lee MY, Park SJ, Park K, Kim KS, Lee H, Hahn SK. Target-Specific Gene Silencing of Layer-by-Layer Assembled Gold-Cysteamine/siRNA/PEI/HA Nanocomplex. *ACS Nano.* 2011; 5:6138–6147. [PubMed: 21739990]
23. Guo ST, Huang YY, Jiang QA, Sun Y, Deng LD, Liang ZC, Du QA, Xing JF, Zhao YL, Wang PC, et al. Enhanced Gene Delivery and siRNA Silencing by Gold Nanoparticles Coated with Charge-Reversal Polyelectrolyte. *ACS Nano.* 2010; 4:5505–5511. [PubMed: 20707386]
24. Akinc A, Goldberg M, Qin J, Dorkin JR, Gamba-Vitalo C, Maier M, Jayaprakash KN, Jayaraman M, Rajeev KG, Manoharan M, et al. Development Of Lipidoid-sirna Formulations For Systemic Delivery To The Liver. *Mol. Ther.* 2009; 17:872–879. [PubMed: 19259063]

25. De Koker S, Hoogenboom R, De Geest BG. Polymeric Multilayer Capsules For Drug Delivery. *Chem. Soc. Rev.* 2012; 41:2867–2884. [PubMed: 22282265]
26. Jain S, Kumar D, Swarnakar NK, Thanki K. Polyelectrolyte Stabilized Multilayered Liposomes For Oral Delivery Of Paclitaxel. *Biomaterials.* 2012; 33:6758–6768. [PubMed: 22748771]
27. Woodrow KA, Cu Y, Booth CJ, Saucier-Sawyer JK, Wood MJ, Saltzman WM. Intravaginal Gene Silencing Using Biodegradable Polymer Nanoparticles Densely Loaded With Small-Interfering RNA. *Nat. Mater.* 2009; 8:526–533. [PubMed: 19404239]
28. Meng H, Mai W, Zhang H, Xue M, Xia T, Lin S, Wang X, Zhao Y, Ji Z, Zink J, et al. Codelivery Of An Optimal Drug/sirna Combination Using Mesoporous Silica Nanoparticles To Overcome Drug Resistance In Breast Cancer In Vitro And In Vivo. *ACS Nano.* 2013; 7:994–1005. [PubMed: 23289892]
29. Stylianopoulos T. EPR-Effect: Utilizing Size-Dependent Nanoparticle Delivery To Solid Tumors. *Ther Deliv.* 2013; 4:421–423. [PubMed: 23557281]
30. Aruffo A, Stamenkovic I, Melnick M, Underhill CB, Seed B. Cd44 Is the Principal Cell-Surface Receptor for Hyaluronate. *Cell.* 1990; 61:1303–1313. [PubMed: 1694723]
31. Ricardo S, Vieira AF, Gerhard R, Leitao D, Pinto R, Cameselle-Teijeiro JF, Milanezi F, Schmitt F, Paredes J. Breast Cancer Stem Cell Markers Cd44, Cd24 And Aldh1: Expression Distribution Within Intrinsic Molecular Subtype. *J. Clin. Pathol.* 2011; 64:937–946. [PubMed: 21680574]
32. Choi CHJ, Alabi CA, Webster P, Davis ME. Mechanism Of Active Targeting In Solid Tumors With Transferrin-Containing Gold Nanoparticles. *Proc. Natl. Acad. Sci. U. S. A.* 2010; 107:1235–1240. [PubMed: 20080552]
33. Park JW. Liposome-Based Drug Delivery In Breast Cancer Treatment. *Breast Cancer Res.* 2002; 4:95–99. [PubMed: 12052251]
34. Koudelka S, Turanek J. Liposomal Paclitaxel Formulations. *J. Controlled Release.* 2012; 163:322–334.
35. Kumar P, Gulbake A, Jain SK. Liposomes A Vesicular Nanocarrier: Potential Advancements In Cancer Chemotherapy. *Crit. Rev. Ther. Drug Carrier Syst.* 2012; 29:355–419. [PubMed: 22876808]
36. Taheri M, Mahjoubi F. MRP1 but not MDR1 is Associated With Response To Neoadjuvant Chemotherapy In Breast Cancer Patients. *Dis. Markers.* 2013; 34:387–393. [PubMed: 23481629]
37. Wei J, Jones J, Kang J, Card A, Krimm M, Hancock P, Pei Y, Ason B, Payson E, Dubinina N, et al. RNA-Induced Silencing Complex-Bound Small Interfering Rna Is A Determinant Of RNA Interference-Mediated Gene Silencing In Mice. *Mol. Pharmacol.* 2011; 79:953–963. [PubMed: 21427169]
38. Boyle P. Triple-Negative Breast Cancer: Epidemiological Considerations And Recommendations. *Ann. Oncol.* 2012; 23(Suppl 6):vi7–vi12. [PubMed: 23012306]
39. Griffiths CL, Olin JL. Triple Negative Breast Cancer: A Brief Review Of Its Characteristics And Treatment Options. *J. Pharm. Pract.* 2012; 25:319–323. [PubMed: 22551559]
40. Jiang G, Park K, Kim J, Kim KS, Hahn SK. Target Specific Intracellular Delivery Of Sirna/pei-Ha Complex By Receptor Mediated Endocytosis. *Mol. Pharm.* 2009; 6:727–737. [PubMed: 19178144]
41. Deng ZJ, Mortimer G, Schiller T, Musumeci A, Martin D, Minchin RF. Differential Plasma Protein Binding To Metal Oxide Nanoparticles. *Nanotechnology.* 2009; 20:455101. [PubMed: 19822937]
42. Deng ZJ, Liang M, Monteiro M, Toth I, Minchin RF. Nanoparticle-Induced Unfolding Of Fibrinogen Promotes Mac-1 Receptor Activation And Inflammation. *Nat. Nanotechnol.* 2011; 6:39–44. [PubMed: 21170037]
43. Deng ZJ, Liang M, Toth I, Monteiro MJ, Minchin RF. Molecular Interaction Of Poly(Acrylic Acid) Gold Nanoparticles With Human Fibrinogen. *ACS Nano.* 2012; 6:8962–8969. [PubMed: 22998416]
44. Deng ZJ, Liang M, Toth I, Monteiro M, Minchin RF. Plasma Protein Binding Of Positively And Negatively Charged Polymer-Coated Gold Nanoparticles Elicits Different Biological Responses. *Nanotoxicology.* 2013; 7:314–322. [PubMed: 22394123]

45. Zhao ZX, Gao SY, Wang JC, Chen CJ, Zhao EY, Hou WJ, Feng Q, Gao LY, Liu XY, Zhang LR, et al. Self-Assembly Nanomicelles Based On Cationic Mpeg-Pla-B-Polyarginine(R-15) Triblock Copolymer For Sirna Delivery. *Biomaterials*. 2012; 33:6793–6807. [PubMed: 22721724]
46. Kumar P, Wu HQ, McBride JL, Jung KE, Kim MH, Davidson BL, Lee SK, Shankar P, Manjunath N. Transvascular Delivery Of Small Interfering Rna To The Central Nervous System. *Nature*. 2007; 448:39–43. [PubMed: 17572664]
47. Appelbaum JS, LaRochelle JR, Smith BA, Balkin DM, Holub JM, Schepartz A. Arginine Topology Controls Escape of Minimally Cationic Proteins from Early Endosomes to the Cytoplasm. *Chem. Biol*. 2012; 19:819–830. [PubMed: 22840770]
48. Liu BR, Huang YW, Winiarz JG, Chiang HJ, Lee HJ. Intracellular Delivery Of Quantum Dots Mediated By A Histidine- And Arginine-Rich Hr9 Cell-Penetrating Peptide Through The Direct Membrane Translocation Mechanism. *Biomaterials*. 2011; 32:3520–3537. [PubMed: 21329975]
49. Morton SW, Herlihy KP, Shopsowitz KE, Deng ZJ, Chu KS, Bowerman CJ, Desimone JM, Hammond PT. Scalable Manufacture of Built-to-Order Nanomedicine: Spray-Assisted Layer-by-Layer Functionalization of PRINT Nanoparticles. *Adv. Mater*. 2013; 25:4707–4713. [PubMed: 23813892]
50. Richardson JJ, Ejima H, Lorcher SL, Liang K, Senn P, Cui J, Caruso F. Preparation Of Nano- And Microcapsules By Electrophoretic Polymer Assembly. *Angew. Chem. Int. Ed. Engl*. 2013; 52:6455–6458. [PubMed: 23657949]



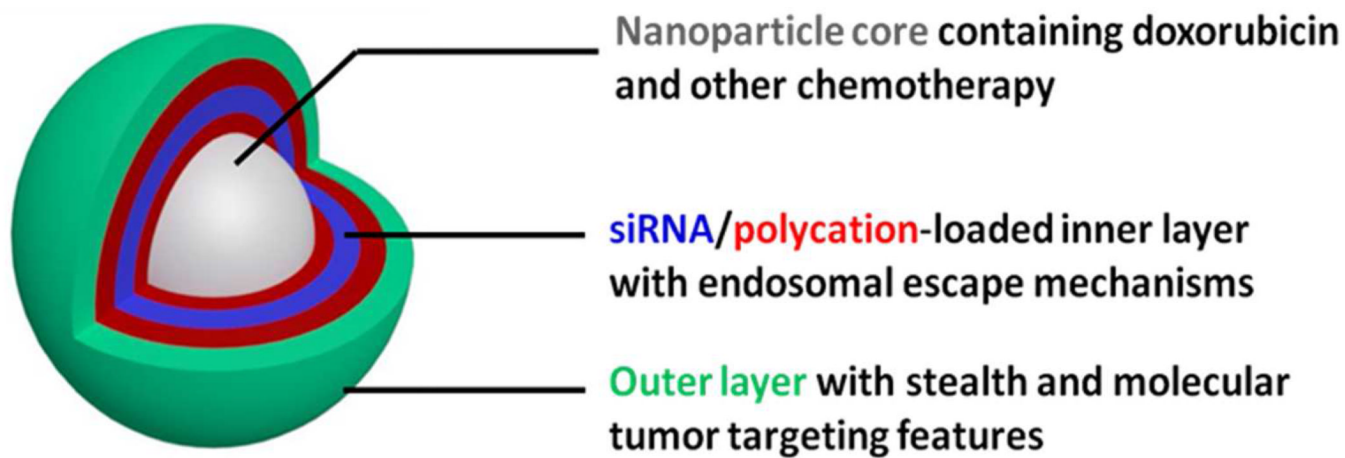


**Figure 1.** Schematic of modular combination drug delivery platform based on the LbL nanoparticles.

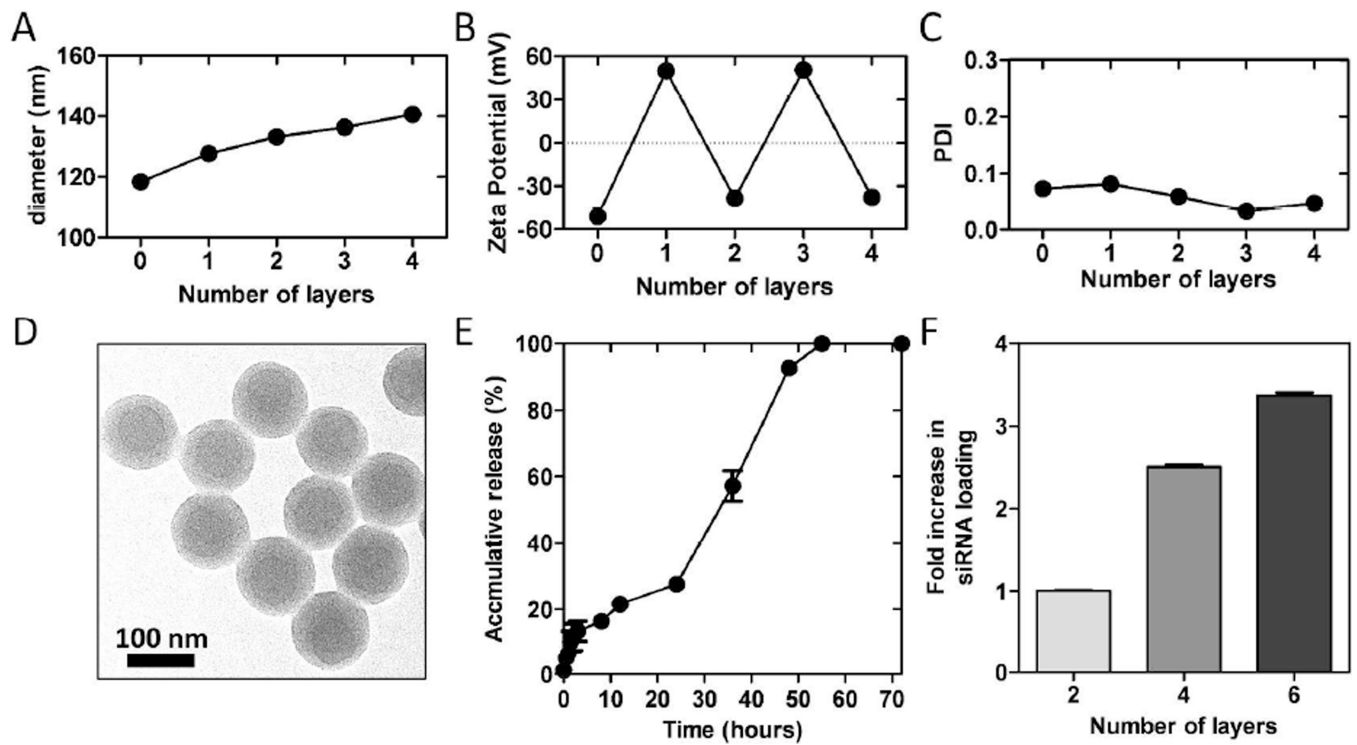


**Figure 2.** Physicochemical characterization of CML/(PLA/siRNA)<sub>n</sub> LbL nanoparticles. Effects of additional layers on (A) hydrodynamic size, (B) zeta potential and (C) polydispersity index (PDI) of the LbL CML nanoparticles. (D) core-shell structure of the LbL CML nanoparticles by transmission electron microscopy. (E) film stability and siRNA release of the nanoparticles in PBS (pH 7.4). (F) Control of siRNA loading by additional layers. The results represent mean  $\pm$  standard deviation ( $n = 3$ ).

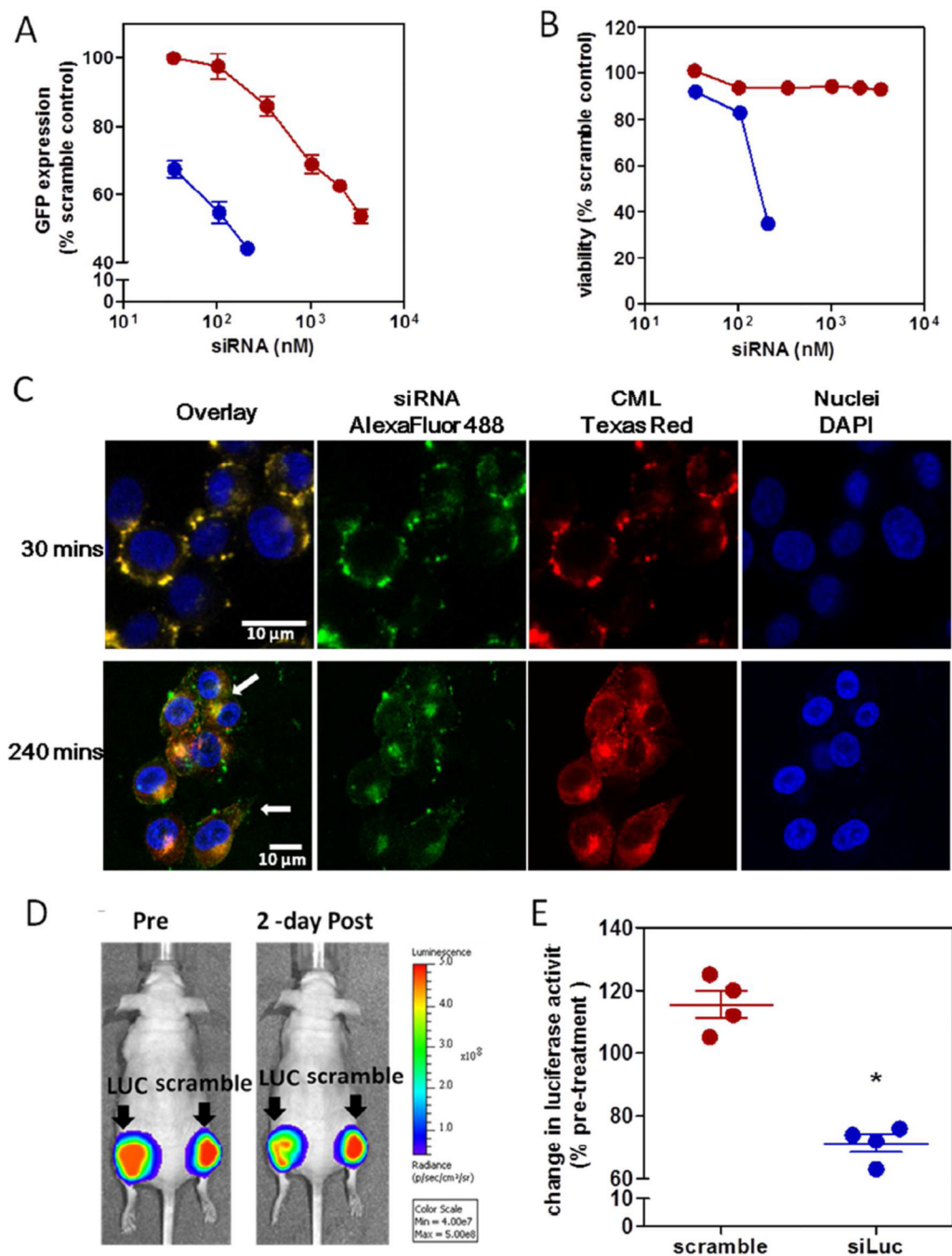


**Figure 3.** Functional characterization of CML/PLA/siRNA/PLA/HA and CML/PEI/siRNA/PEI/HA LbL nanoparticles *in vitro* and *in vivo*. (A) GFP expression knockdown and (B) cytotoxicity of PLA/siRNA LbL nanoparticle treatment (red dots and line) or PEI/siRNA LbL nanoparticle treatment (blue dots and line) in GFP-expressing MDA-MB-468 cells. The treatments were standardized to siRNA concentrations. The Scrambled siRNA was used as negative controls ( $n = 3$ ,  $P < 0.05$ ). (C) Confocal microscopic analysis of intracellular trafficking of PLA/siRNA LbL nanoparticles using AlexaFluor488-labeled siRNA and TexasRed labeled CML cores 30 minutes- and 4 hours-post incubation with MDA-MB-468

cells. (D) Live animal bioluminescence analysis of *firefly* luciferase-expressing MDA-MB-468 subcutaneous xenograft-bearing nude mice before and 2 days after treated with a single-dose of 1 mg/kg intratumorally injected luciferase-targeting siRNA LbL nanoparticles at the left flank tumors and the scrambled-siRNA LbL nanoparticles at the right flank tumors. (E) Comparison of luciferase activities in the tumors 2 days after treated with the luciferase siRNA or the scrambled siRNA. The results represent mean  $\pm$  standard deviation ( $n = 4$ ,  $P < 0.05$ ).

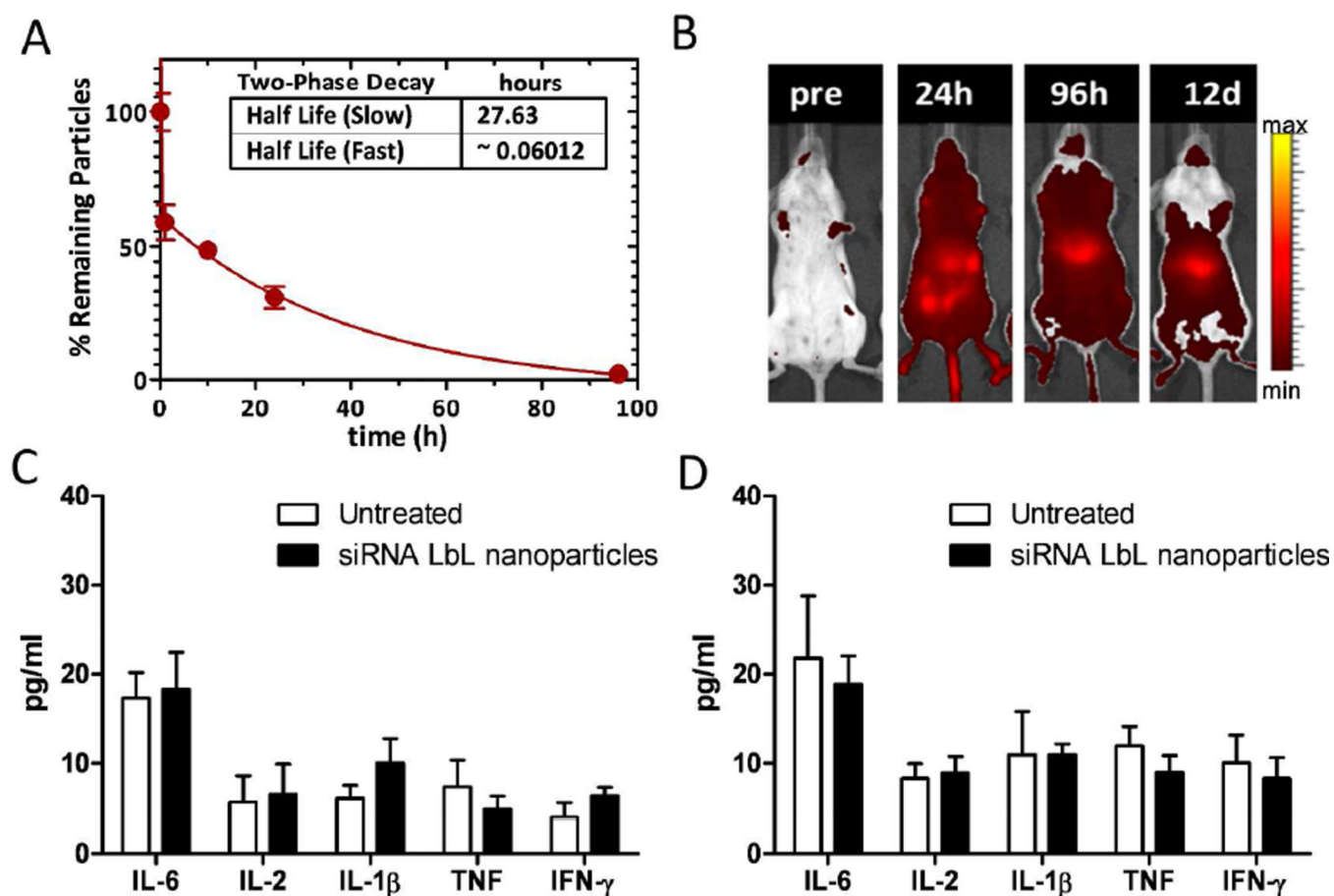


**Figure 4.** Pharmacokinetics and immunogenicity analysis of intravenously administered CML/PLA/siRNA/PLA/HA LbL nanoparticles at 1 mg/kg siRNA in healthy BALB/c mice. Nanoparticle cores were fluorescently labeled with AlexaFluor677 to assess (A) blood half life in blood specimen and (B) biodistribution using live animal fluorescent imaging ( $n = 4$ ). To evaluate the immunogenicity, mouse sera were collected (C) 4 hours and (D) 24 hours post-injection. Interleukin (IL)-6, IL-2, IL-1 $\beta$ , tumor necrosis factor (TNF) and interferon (IFN)- $\gamma$  were measured by BD<sup>TM</sup> Cytometric Bead Arrays. The results represent mean  $\pm$  standard deviation ( $n = 3$ ).

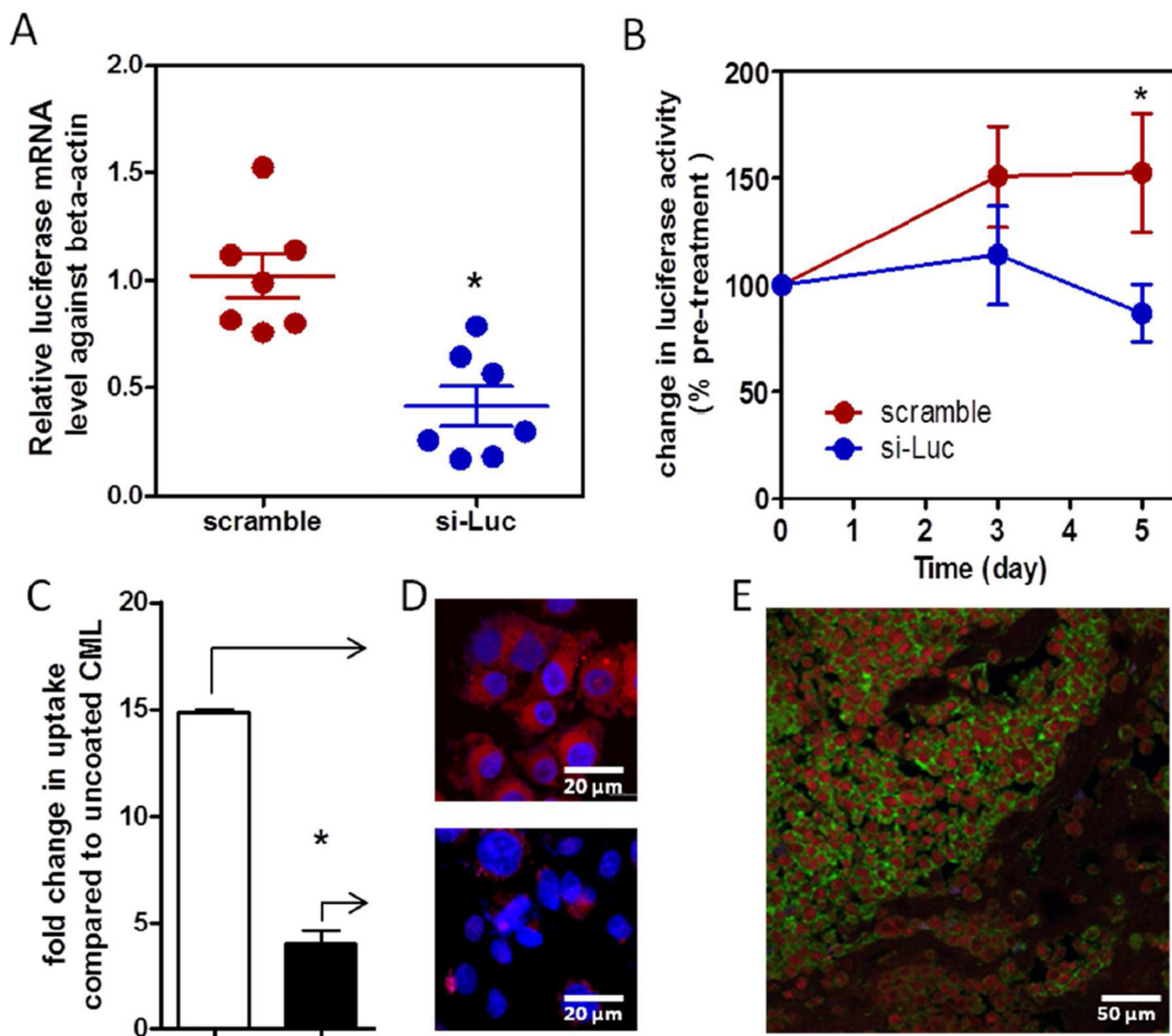


**Figure 5.** Systemic delivery of siRNA using CML/PLA/siRNA/PLA/HA LbL nanoparticles in mice models. (A) Luciferase mRNA level and (B) bioluminescence activities in subcutaneous MDA-MB-468 tumors of the nude mice treated with a single dose tail vein injection of 1.4 mg/kg luciferase-targeting siRNA-loaded LbL nanoparticles, and compared with the scrambled siRNA control ( $n = 7$ ,  $(*) P < 0.05$ ). (C) Flow cytometry and (D) confocal microscopic analyses of uptake of HA-coated LbL nanoparticles (open bar in C, upper panel in D (nanoparticles in red, nuclei in blue)) in MDA-MB-468 cells *in vitro*, and compared with the addition of excess free HA at 100  $\mu\text{g}/\text{ml}$  (closed bar in C, lower panel in D). The results represent mean  $\pm$  standard deviation ( $n = 3$ ,  $P < 0.05$ ). (E) Immunofluorescence analysis of tumor tissue section isolated from the mice treated with the siRNA-loaded LbL nanoparticles (CD44 in red, nanoparticles in green and nuclei in blue).

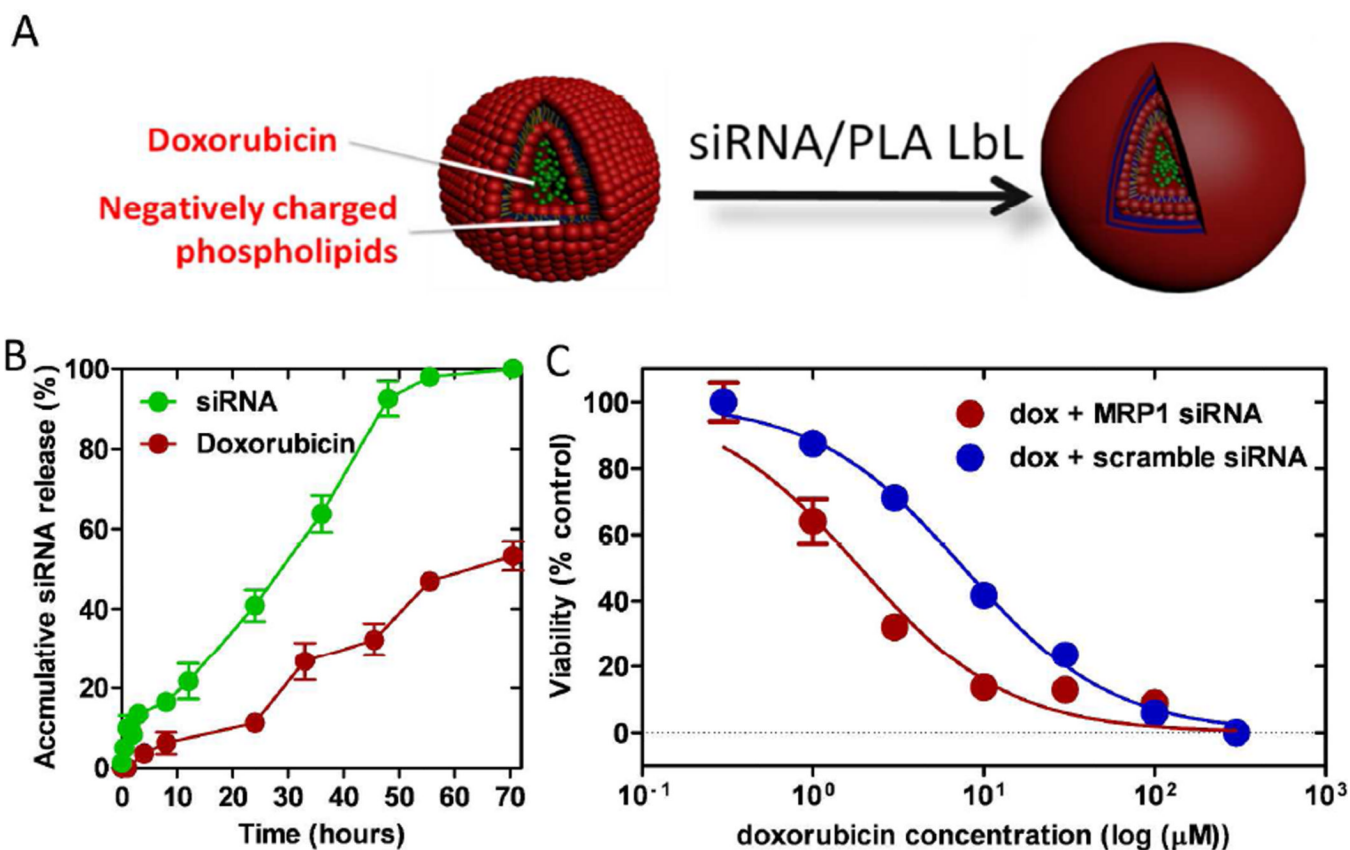


**Figure 6.**

The co-delivery of siRNA and doxorubicin using the modular Dox-liposome/PLA/siRNA/PLA/HA LbL nanoparticle platform. (A) Design schematics of the siRNA-doxorubicin LbL liposomes. (B) Release profile of the two therapeutics components: siRNA and doxorubicin from the LbL liposomal nanoparticles in DMEM tissue culture medium over 72 hours ( $n = 3$ ). (C) Examination of the siRNA-enhanced cytotoxicity of the combo therapy in MDA-MB-468 cells. The results represent mean  $\pm$  standard deviation ( $n = 3$ ,  $P < 0.05$ ).

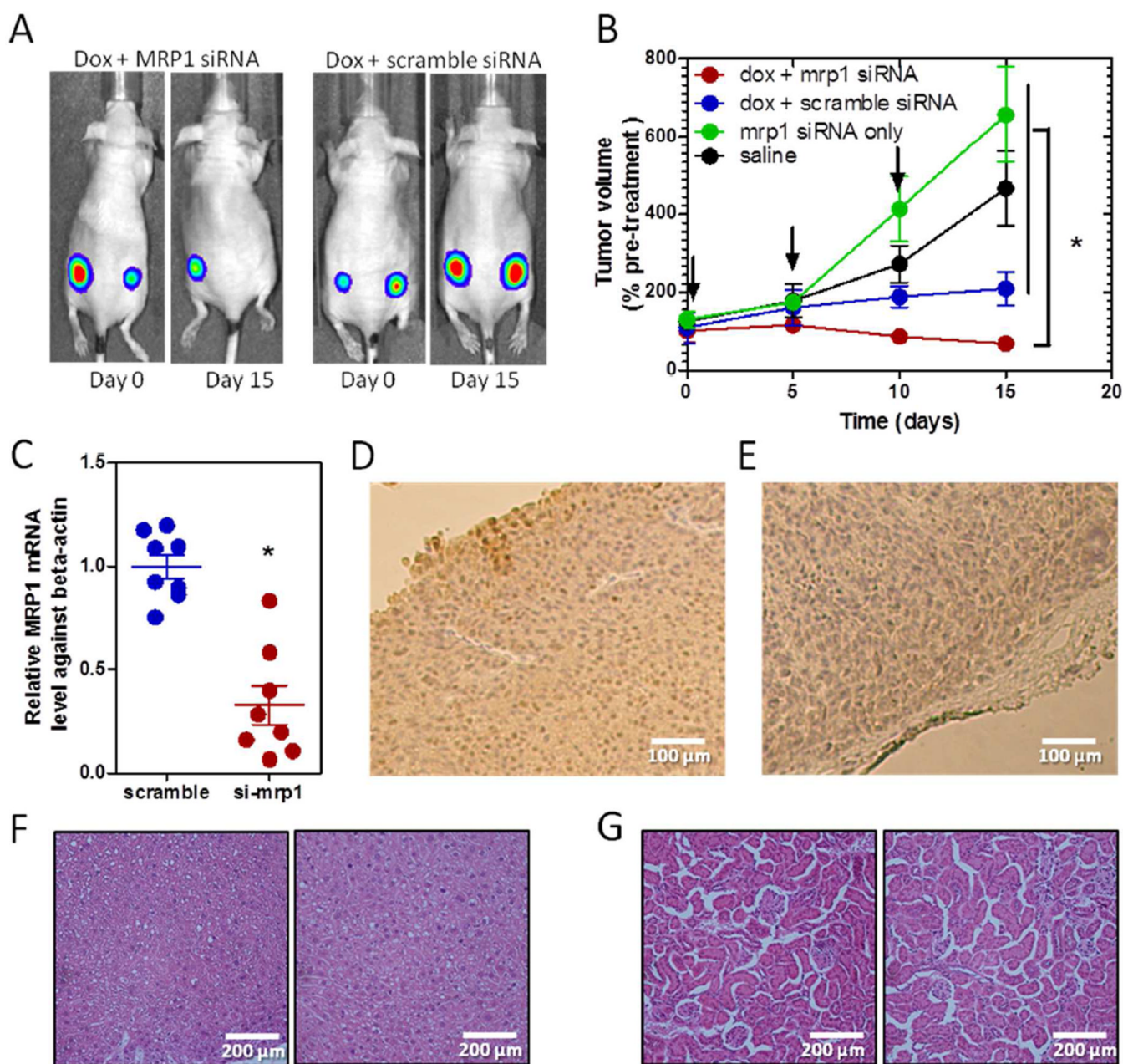


**Figure 7.** Assessment of codelivery of MRP1 siRNA and doxorubicin using Dox-liposome/PLA/siRNA/PLA/HA LbL liposomes for combination therapy to TNBC in mice models. (A, B) Change in tumor volume in nude mice bearing subcutaneous MDA-MB-468 xenografts treated with the MRP1 siRNA doxorubicin LbL liposomes, compared to singlecomponent therapy and untreated controls. The mice were treated through repeated tail vein injection at 1 mg/kg siRNA and/or doxorubicin on day 0, 5, and 10 (marked by arrows). The tumor volume was monitored by luciferase bioluminescence ( $n = 6-8$ , (\*)  $P < 0.05$ ). (C) Quantitative RT-PCR analysis of MRP1 mRNA level in tumor tissue isolated from mice treated with the combo therapies, compared with the dox + scramble siRNA control. The results represent mean  $\pm$  standard deviation ( $n = 8$ , (\*)  $P < 0.05$ ). Immunohistochemistry analysis of MRP1 protein expression in tumor tissues isolated from (D) saline-treated mice



and (E) siRNA/dox-treated mice. Histology analysis of H&E-stained (F) liver and (G) kidney tissue sections isolated from the mice of the combo treatment group (left panels) and the saline-treated control group (right panels).

**Table 1**

Serum levels of AST, ALT, BUN and creatinine at the end of the 15-day treatment in MDA-MB-468 xenograft model.

|                 | AST U/I  | ALT U/I | BUN mg/dl | Creatininemg/dl |
|-----------------|----------|---------|-----------|-----------------|
| Control         | 193±3    | 42 ± 5  | 32 ± 4    | 0.4 ± 0.1       |
| siMRP1 only     | 242 ± 5  | 34 ± 4  | 32 ± 1    | 0.3 ± 0.1       |
| Dox + scramble  | 190 ± 24 | 67 ± 10 | 26 ± 1    | 0.2 ± 0.2       |
| Dox + siMRP1    | 163 ± 52 | 72 ± 7  | 27 ± 6    | 0.3 ± 0.2       |
| Reference range | 54–298   | 17–77   | 8–33      | 0.2–0.9         |

Data are mean ±SD (*n* =3 per group).

ALT, alanine aminotransferase; AST, aspartate aminotransferase; BUN, blood urine nitrogen; dox, doxorubicin; scramble, scrambled-sequence siRNA; siMRP1, MRP1 targeting siRNA.